Rigorous Analysis of Hysteresis Structure Observed in Arnol'd Tongue

Mizuki Urushibara[†], Tadashi Tsubone[‡], and Naohiko Inaba[⋆]

†‡ Nagaoka University of Technology, 1603-1, Kamitomioka, Nagaoka, Niigata, 940-2188, Japan
⋆ Shonan Institute of Technology, 251-8511, Fujisawa, Kanagawa, Japan
Email: † s203128@stn.nagaokaut.ac.jp, ‡ tsubone@vos.nagaokaut.ac.jp, ⋆ naohiko@yomogi.jp

Abstract—This study investigates Arnol'd tongues generated by 2-D piecewise-constant driven oscillator. In this paper, we derived analytically some of the bounds of the fundamental harmonic entrainment region for increasing time period T. We also confirmed the transitions from the periodic attractor to the two chaotic attractors and then to the other periodic attractor.

1. Introduction

Forced synchronization phenomena are often observed in biology and engineering systems[1, 2]. The region where forced synchronisation occurs is known the Arnol'd tongue, and the analysis of it has been actively research in recent years because of its importance in understanding forced synchronization. It is worth noting that Szalei and Osinga [3, 4] have succeeded in deriving Arnol'd tongue bifurcation boundaries explicitly in stick-slip oscillator. We have also analytically derived the boundary of Arnol'd tongue in autonomous piecewise linear oscillator and 2-D piecewise-constant oscillator[5, 6].

In previous researches, we introduced a deriving algorithm for rigorous solutions of 2-D piecewise-constant driven oscillator that has piecewise linear solutions. We have used the algorithm to derive the inner to outer boundary of Arnol'd tongue analytically. However, the hysteresis structure of the Arnol'd tongue has not been fully discussed yet.

Therefore, in this paper, we analytically derive the boundaries of Arnol'd tongue when the parameters are varied from outside to inside. We also investigate the bifurcation phenomenon that occurs in this case. Some typical bifurcation phenomena are confirmed in laboratory experiments.

ORCID iDs First Author: [iD]0000-0002-3616-4467, Second Author: [iD]0000-0001-7457-4232, Third Author: [iD]0000-0003-1153-7025

Figure 1: 2-D Piecewise-constant Driven Oscillator.

$$i_i = I_i \cdot H(v_i) \qquad i_i = I_i \cdot sgn(v_i)$$

(a) Hysteresis characteristic. (b) Signum function.

Figure 2: Symbols and nonlinear characteristics

$$i_i = I_i \cdot B(T, t)$$
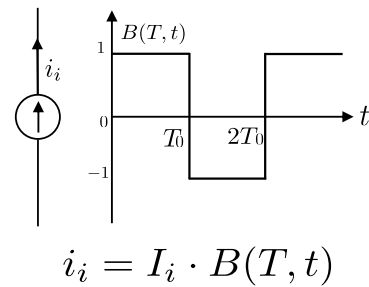
Figure 3: Waveform of the rectangular periodic current source.

2. 2-D Piecewise-constant Driven Oscillator

Figure 1 shows a circuit model of the 2-D piecewise-constant driven oscillator analyzed in this study. In the figure, $H_1(v_1)$ and $H_2(v_1)$ are hysteresis characteristic shown in Fig. 2a and $Sgn(v_2)$ is a signum function (see Fig. 2b). In addition, $B(T, t)$ rep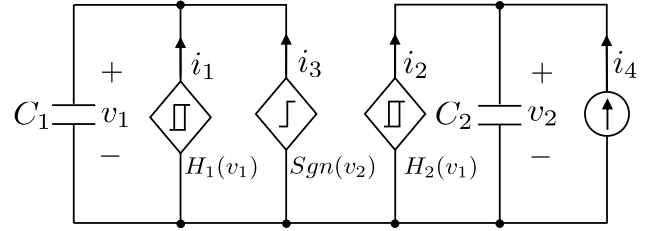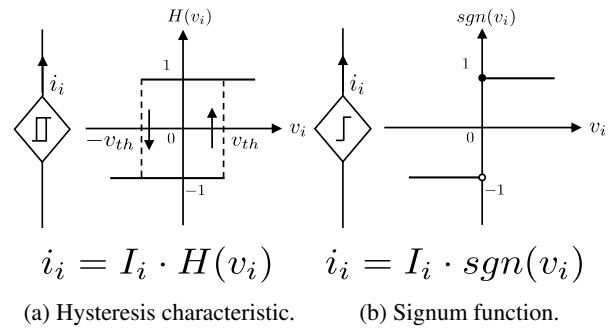resents a rectangular wave current source, as shown in Fig. 3. The governing equation of this circuit is described as follows:

$$\begin{cases} C_1 \dfrac{dv_1}{dt} = I_1 \cdot H_1(v_1) + I_3 \cdot Sgn(v_2), \\ C_2 \dfrac{dv_2}{dt} = I_2 \cdot H_2(v_1) + I_4 \cdot B(T_0, t). \end{cases} \quad (1)$$

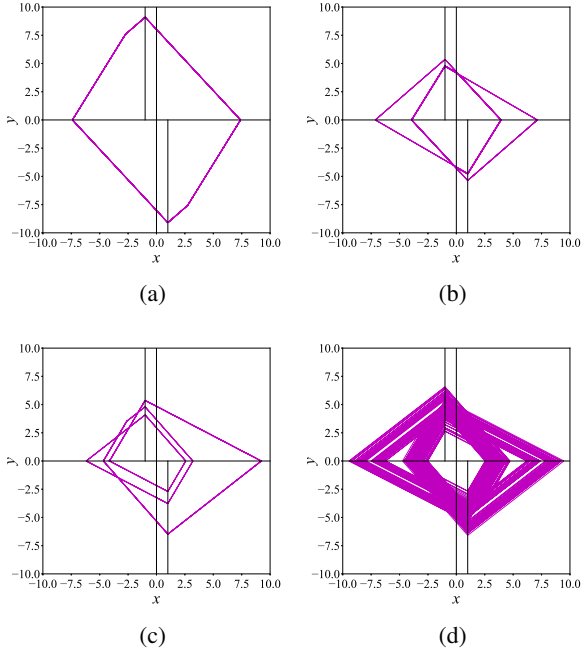We consider following conditions for generates oscillations.

(a)

(b)

(c)

(d)

Figure 4: Attractors obtained from rigorous solution algorithm simulations, (a) periodic solution in the fundamental harmonic entrainment region ($\alpha \cong 0.2, \beta \cong 0.3, T \cong 15$), (b) periodic solution in the 1/3-subharmonic entrainment region ($\alpha \cong 0.2, \beta \cong 0.3, T \cong 30$), (c) chaos attractor ($\alpha \cong 0.2, \beta \cong 0.37, T \cong 30$.), (d) chaos attractor ($\alpha \cong 0.2, \beta \cong 0.378, T \cong 30$).

$$I_2 = -I_3, I_1 \cdot I_2 < 0. \tag{2}$$

Here, using the following normalized variables and parameters

$$\tau = \frac{I_2}{C_1 v_{th}}, \quad x = \frac{1}{v_{th}} v_1, \quad y = \frac{C_2}{C_1 v_{th}} v_2,$$

$$\alpha = -\frac{I_1}{I_2}, \quad \beta = \frac{I_4}{I_2}, \quad T = \frac{I_2}{C_1 v_{th}} T_0, \tag{3}$$

Eq. (1) is normalized as follows:

$$\begin{cases} \dot{x} = -\alpha \cdot h(x) - sgn(y), \\ \dot{y} = h(x) + \beta \cdot B(T, \tau), \end{cases} \tag{4}$$

where " $\cdot$ " denotes differentiation with normalized time τ and $h(x)$ is the normalized hysteresis. In order to oscillate, the following conditions are also assumed

$$0 < \alpha < 1 \quad \text{and} \quad 0 < \beta < 1. \tag{5}$$

The attractors observed in the experiment are shown in Fig. 5.
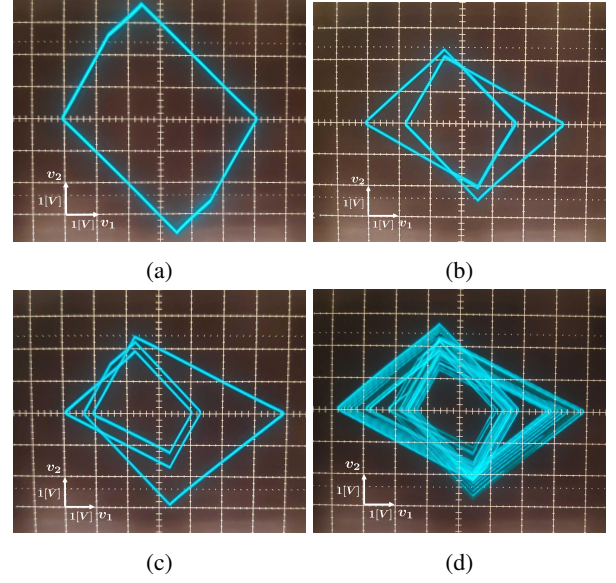

(a)

(b)

(c)

(d)

Figure 5: Attractors observed in the experiment, (a) periodic solution in the fundamental harmonic entrainment region ($\alpha \cong 0.2, \beta \cong 0.3, T \cong 15$), (b) periodic solution in the 1/3-subharmonic entrainment region ($\alpha \cong 0.2, \beta \cong 0.3, T \cong 30$), (c) chaos attractor ($\alpha \cong 0.2, \beta \cong 0.37, T \cong 30$.), (d)chaos attractor ($\alpha \cong 0.2, \beta \cong 0.378, T \cong 30$).

3. Bifurcation Phenomena

We use the rigorous solution algorithm proposed by Kuriyama et al. [6]. This method is based on the idea that since the circuit model of this study is piecewise linear behavior, the rigorous solution can be obtained by considering the map from a boundary to other boundary where the vector field transitions. We focus on the period T of the external input and define the Poincaré map as follows:

$$S_p = \{(x, y, \tau) | \tau = nT\}, \tag{6}$$

$$\boldsymbol{F_p} : S_p \rightarrow S_p, \tag{7}$$

$$(x_n, y_n, nT) \mapsto (x_{n+1}, y_{n+1}, (n+1)T). \tag{8}$$

The fixed point is determined by

$$(x_n, y_n, (n+m)T) = \boldsymbol{F_p^m}(x_n, y_n, nT), \tag{9}$$

where m is the period.

3.1. Boundary of Arnol'd tongue when T is increased

We investigate outer to inner boundary of the fundamental harmonic entrainment region. Figure 6 shows the boundary of the fundamental harmonic region when the parameter is varied from the outside to the inside. Furthermore, the attractors observed in the neighborhood of the boundary are shown in Fig. 7. As a simple example, consider the attractor in Fig. 7a. First, derive the fixed point from Eq. (9). A bifurcation occurs when the fixed point
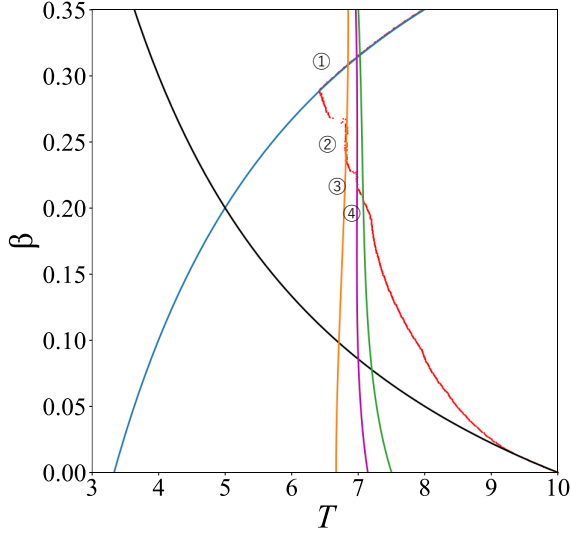
Figure 6: Boundary of the fundamental harmonic entrainment region. Red dots are simulation results when T is moved from outside to inside the fundamental harmonic entrainment region. Black line is the boundary from the inside to the outside of the fundamental entrainment harmonic region. The blue, yellow, purple, and green lines are analytically derived boundaries from the respective attractors in Fig. 7.

(a) ① in Fig. 6 ($\alpha \cong 0.2, \beta \cong 0.30, T \cong 6.0$).
(b) ② in Fig. 6 ($\alpha \cong 0.2, \beta \cong 0.26, T \cong 6.75$).

(c) ③ in Fig. 6 ($\alpha \cong 0.2, \beta \cong 0.226, T \cong 6.96$).
(d) ④ in Fig. 6 ($\alpha \cong 0.2, \beta \cong 0.209, T \cong 7.0$).

Figure 7: Attractors observed in the neighborhood of outer to inner boundary.

collides with the boundary $y = 0$ where the $sgn(y)$ function switches. Therefore, from $y_n = 0$, the bifurcation boundary is
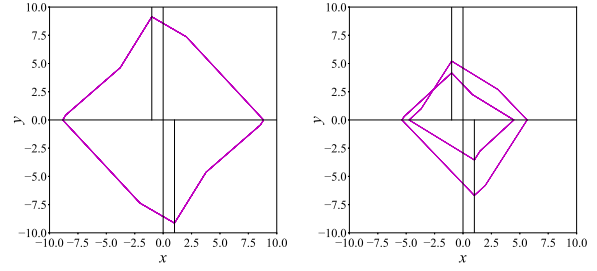
$$T = -\frac{2}{\beta - 3\alpha}. \tag{10}$$

This bifurcation is a saddle-node bifurcation because the stable fixed point and the unstable fixed point collide at $y_n = 0$.
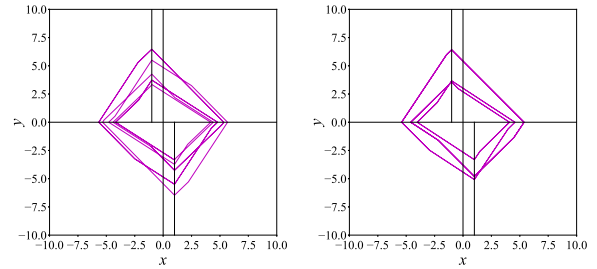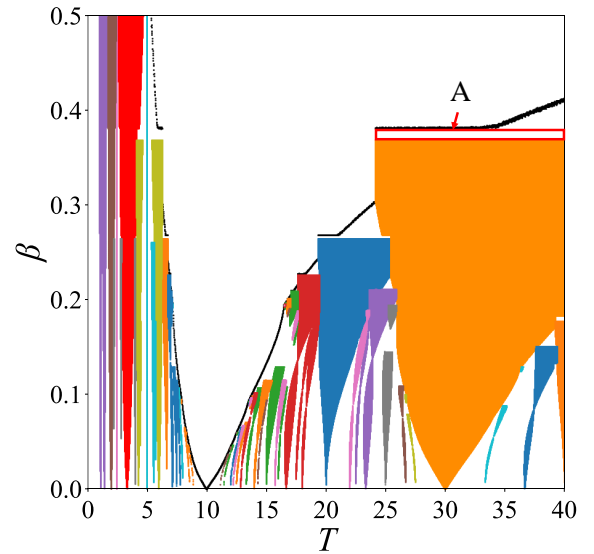
The solid line in Fig. 6 shows the derivation of the bifurcation boundary in the same way. Each solid line which is the derived boundaries agrees with the red dots observed by the brute force method.

3.2. Bifurcation phenomenon when β is increased

Figure 8 shows the bifurcation diagram for increasing β. The largest Lyapunov exponent in the neighborhood of region A, where the transition from periodic to chaotic and then to periodic solutions is shown in Fig. 9. When $\beta \cong 0.368$, the largest Lyapunov exponent exceeds 0 and the attractor transits chaos. The attractors before and after the transition are shown in Fig. 10,11. The bifurcation occurs and the transition is made to either of the chaotic attractors in Fig. 11. This structure is similar to a pitchfork bifurcation. However, different from the pitchfork bifurcation that occurs in a smooth system, this bifurcation is named a non-smooth pitchfork bifurcation because the transition to the attractor occurs abruptly after the bifurcation.

Figure 8: Bifurcation diagram with increasing β. The region surrounded by the black dots are the fundamental harmonic entrainment region. Orange region is the 1/3-subharmonic entrainment region. Blue region is the 1/2-subharmonic entrainment region. The region A is transitioning from periodic to chaotic and then to periodic solutions.

Next, we consider the change from chaos to periodic solutions. As shown as Fig. 9, when beta = 0.378, the at-

tractor will be rapidly attracted to periodic solution from chaotic one. This suggests that a crisis has occurred.
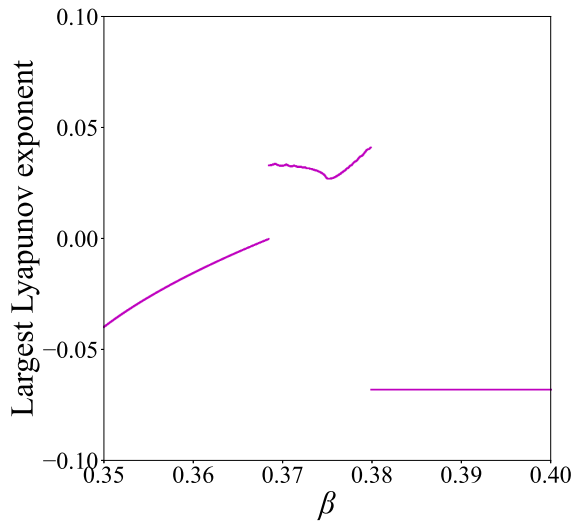

Figure 9: The largest Lyapunov exponent in the neighborhood of region A ($T = 30$).
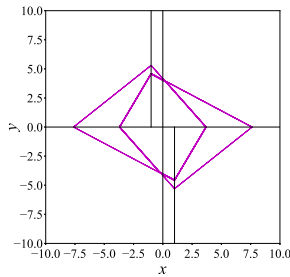

Figure 10: Periodic solution before transition ($\alpha \cong 0.2, \beta \cong 0.36, T \cong 30$).
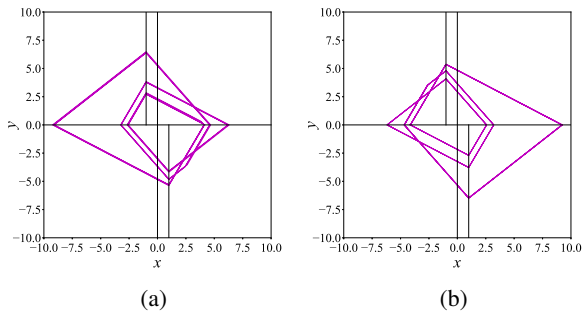

Figure 11: Chaos attractors after transition ($\alpha \cong 0.2, \beta \cong 0.37, T \cong 30$), (a) initial condition ($x = -4.0, y = 0.5$), (b) initial condition ($x = -4.0, y = -0.5$).

4. Conclusion

In this paper, we considered Arnol'd tongues of 2-D piecewise-constant driven oscillator. By using analysis with rigorous solution, we derived analytically some of the boundaries of the fundamental harmonic entrainment for increasing T. Furthermore, the transition from the periodic solution to the two chaotic attractors and then back to the periodic solution is confirmed.

Now we are attempting to derive analytically boundaries for transition from chaotic attractors to periodic solution.

References

[1] K. Tsumoto, T. Yoshinaga, H. Iida, H. Kawakami, K. Aihara, "Bifurcations in a mathematical model for circadian oscillations of clock genes," Journal of Theoretical Biology 239, pp. 101-122, 2006.

[2] Inaba N, Kamiyama K, Kousaka T, Endo T. "Numerical andexperimental observation of Arnol'd resonance webs in an electricalcircuit," Physica D 311–312:17–24, 2015.

[3] Zh.T. Zhusubaliyev, E.A. Soukhoterin, and E. Mosekilde, "Border-collision bifurcations on a two-dimensional torus, " Chaos Solitons Fractals 13, pp.1889–1915, 2002.

[4] R. Szalai and H.M. Osinga, "Arnol'd tongues arising from a grazing-sliding bifurcation, " SIAM J. Appl. Dyn. Syst. 8, pp.1434–1461, 2009.

[5] Viet Duc Le, Tadashi Tsubone, and Naohiko Inaba, "Rigorous analysis of Arnol'd Tongues in a Manifold Piecewise-linear Circuit, " IEEJ Trans., vol 15, pp.1070-1076, 2020.

[6] Hironori Kuriyama and Tadashi Tsubone, "Arnold tongues of 2-D Piecewise Constant Driven Oscillator," Proc. of 2015 International Symposium on Nonlinear Theory and its Applications (NOLTA2015), pp. 479-482, 2015.